Iron based Metal-organic Frameworks and their Polymer Composites for Sustainable Delivery of Herbicides

Parimal C. Bhomick,[a,b] Evdokiya H. Ivanovska,[c] Lila A. M. Mahmoud,[d] Huan V. Doan,[e] Lui R. Terry,[a] Matthew A. Addicoat,[f] Jemma L. Rowlandson,[g] Sebastien Rochat,[h] Valeska P. Ting,[e,*] Sanjit Nayak[a,*]

a. University of Bristol, Bristol Composite Institute, School of Civil, Aerospace and Design Engineering Queen's Building, University Walk, Bristol, UK BS8 1TR
b. Nagaland University - Lumami Campus, Department of Chemistry; Nagaland University, Lumami, Nagaland, IN 798627
c. University of Bradford, School of Archaeological and Forensic Sciences, Bradford, West Yorkshire, UK BD7 1DP
d. University of Bristol, School of Chemistry, BS8 1TS, Bristol, UK BS8 1TS
e. Australian National University, School of Chemistry, Canberra, ACT, AU 2601
f. Nottingham Trent University, Chemistry and Forensics, Clifton Lane, Nottingham, UK NG11 8NS,
g. University of Bristol, Department of Mechanical Engineering, Queen's Building, University Walk, Bristol, UK BS8 1TR
h. University of Bristol, School of Engineering Mathematics and Technology, University of Bristol, Bristol, UK BS8 1TR

KEYWORDS. Metal-organic frameworks (MOFs); MIL-101(Fe); biodegradable composites; agrochemical delivery; sustainable agriculture

ABSTRACT: Sustainable agriculture will play a key role to ensure food security for the rising global population. Controlled and precision delivery of agrochemicals such as herbicides and pesticides play a critical role towards sustainable agriculture. Recently, porous metal-organic frameworks (MOFs) have shown promising results for controlled agrochemical delivery. Because of their low toxicity and biocompatibility iron-based metal-organic frameworks (Fe-MOFs) are highly suitable for applications in agriculture over many other MOFs. In this study, two iron-based MOFs, MIL-101(Fe) and NH_2-MIL-101(Fe), and their biodegradable polymer composites were studied for controlled herbicide delivery. Two herbicides, 2,4-dichlorophenoxyacetic acid (2,4-D) and 2-methyl-4-chlorophenoxyacetic acid (MCPA), were post synthetically loaded into these two Fe-MOFs and incorporated into biodegradable polycaprolactone (PCL) matrix to form composite membranes for ease of handling and delivery. MIL-101(Fe) showed loading capacities of 18.06 wt% and 21.51 wt%, respectively for 2,4-D and MCPA, while for NH_2-MIL-101(Fe) the loading capacities for the same herbicides were 26.61 wt% and 23.32 wt%. Despite high loading capacity, both MOFs showed certain degree of degradation during the herbicide loading. The release of 2,4-D and MCPA from MIL-101(Fe) and NH_2-MIL-101(Fe) and their PCL composites were studied using UV-visible spectroscopy over a nine-day period. NH_2-MIL-101(Fe) and its PCL composite demonstrated slower and more controlled release profiles of the herbicides than MIL-101(Fe) and its composites. The results were also corroborated by computational studies which showed stronger interaction of the herbicides with NH_2-MIL-101(Fe).

1. INTRODUCTION

The use of agrochemicals such as pesticides and herbicides are essential in modern agriculture as we race to keep up with global food demand. However, their accumulation in the environment, along with their degradation products, pose great threat to the environment, human health and wider ecosystem. This include contamination of groundwater and food chains, which can lead to severe health issues such as cancer, neurological disorders, immunological issues, and reproductive defects.[1] Several pesticides and other agrochemicals have been under scrutiny because of their associated toxicity, but remain in use as they are essential for maintaining crop productivity and global food demands.[2-4] Pesticides are mainly delivered by conventional methods such as blanket spraying over large vegetation areas. These methods use a very high initial delivery dose (up to 500 L/ha)[5], and it is estimated that only 0.1% of the applied pesticides reach the intended target. The rest of the dose enter the environment directly through air, water, and soil, directly contributing towards high level of ecotoxicity.[6-10] It is therefore essential that a controlled release technology is developed for more targeted and environmentally friendly pesticide delivery. Many approaches, such as chemical degradation, membrane filtration, microbial treatment and adsorption have been investigated to address these issues and lessen the environmental impact.[11] Out of these methods, adsorption has outperformed the others as it offers a simpler and more effective way to extract pesticides.[12-14] Several elements need to be considered for an effective adsorption process, including the adsorbent's high porosity, surface area, and interaction with the adsorption sites. In this regard, metal-organic frameworks (MOFs) serve as an ideal candidate. Metal-organic frameworks are a class of materials made of metal ions/clusters connected with organic linkers, often forming crystalline 2D or 3D networks presenting permanent porosity. Compared to traditional adsorbents, MOFs offer several advantages, including high surface area, high and tuneable porosity, and easy post-synthetic modification for tailored host-guest interactions. Due to their high uptake capacity and selective adsorption, MOFs have been extensively studied for the removal and sensing of agrochemicals.[15] Moreover, MOFs can serve as delivery platforms for agrochemicals, representing an emerging area of study with growing interest.[11]

Among the plethora of MOFs synthesized to date, iron-based MOFs (Fe-MOFs) stand out as excellent candidates for agricultural applications because of their cost-effectiveness, and environmental friendliness allowing these MOFs to serve dual functions: (a) as hosts for agrochemicals for controlled delivery and (b) as a micronutrient source for plant growth.[11, 16] MIL-101(Fe)[17, 18] is a mesoporous Fe-MOF with pore dimensions of 12 Å × 29 Å and 16 Å × 34 Å, composed of non-toxic components, making it a relatively ecofriendly[16] and biocompatible[19, 20] MOF suitable for agricultural applications.

However, the crystalline and often powdery form of pristine MOFs including MIL-101(Fe) poses a challenge for their handling, transport, and practical applications. To overcome this barrier, the crystalline MOFs can be incorporated into polymer composites. Such hybrid MOF/polymer composites can improve handling, transport, and overall versatility, expanding their scope for potential applications.[21, 22] Polycaprolactone (PCL) was selected as the polymer matrix for this study due to its biocompatibility and non-toxicity.[23] Its superior mechanical properties,[24] along with a relatively slow hydrolytic degradation rate compared to other biodegradable polymers like polylactic acid, make PCL an ideal candidate for fabricating polymer composites for agrochemical delivery.[25]

In this study, two non-toxic and biocompatible MOFs (MIL-101(Fe) and NH_2-MIL-101(Fe), were synthesized and loaded with two herbicides, 2,4-dichlorophenoxyacetic acid (2,4-D), and 2-methyl-4-chlorophenoxyacetic acid (MCPA), as model agrochemicals. These herbicides are widely used for broadleaf weed control in both crop and non-crop lands due to their effective herbicidal activities. Subsequently, these loaded MOFs were integrated into a biodegradable polymer (polycaprolactone) to form MOF-based composite membranes for the controlled release of 2,4-D and MCPA (Scheme 1). As illustrated in Scheme 1, these biodegradable membranes can be activated by irrigation water or rain, releasing agrochemicals at a controlled rate.

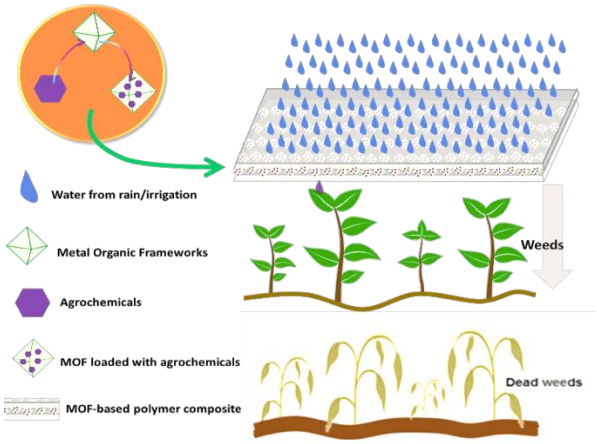

Scheme 1. Illustration of MOF-based polymer composite for delivery of agrochemicals and pesticides.

This enhances the targeted delivery and reduces the overuse of agrochemicals. Due to biocompatibility of the iron-based MOFs and the biodegradability of PCL, the composite would eventually degrade, and the iron from the MOFs can be utilized as a micronutrient replenishment, making the process sustainable.

2. MATERIALS AND METHODS

2.1. Material used. Iron (III) chloride hexahydrate (ACS reagent, 97%), terephthalic acid (98%), 2-amino terephthalic acid (99%) and the herbicides (≥95.0%) were purchased from Sigma-Aldrich, dimethylformamide, and ethanol were purchased from Fischer Chemicals. Polycaprolactone (Mol. Wt. ~80,000) was purchased from Acros Organics. All chemicals were used as received without any further purification.

2.2. Synthesis of MIL-101(Fe). For the synthesis of MIL-101(Fe), a solvothermal approach was used. 0.412 g (2.48 mmol) of 1,4-benzenedicarboxylic acid and 1.3244 g (4.9 mmol) of $FeCl_3 \cdot 6H_2O$ were dissolved in 30 mL of DMF by sonication for 20 minutes in a Teflon-lined vial. The mixture was heated to 110 °C at a heating rate of 5°C/min, maintained at 110 °C for 20 hours and cooled to room temperature at 0.5°C/min. The orange product was collected by centrifugation (4500 rpm, 20 min) and washed with DMF and ethanol for 3 times to remove unreacted compounds and then dried at 60°C for 20 h under vacuum. The colour of the final product was light orange.

2.3. Synthesis of NH_2-MIL-101-Fe. For the synthesis of NH_2-MIL-101-Fe, 2-amino terephthalic acid (0.449 g, 2.48 mmol) and $FeCl_3 \cdot 6H_2O$ (1.3244 g, 4.9 mmol) were dissolved in a Teflon-lined vial by sonication at 25 °C for 20 minutes. The mixture was heated to 110 °C at a heating rate of 5°C/min, maintained at 110 °C for 20 hours and cooled to room temperature at 0.5°C/min. The dark brown powder was collected by centrifugation (4500 rpm, 20 min) and washed with DMF and ethanol for 3 times to remove unreacted compounds and then dried at 60 °C for 20 h under vacuum.

2.4. Preparation of Polycaprolactone-MOF Composites. In a 50 mL round bottom flask, 200 mg of polycaprolactone polymer (PCL) was let to dissolve in 15 mL chloroform by stirring the mixture for 30 min at 800 rpm. In a 10 mL glass vial, 5 mL of PCL solution was added to 5 mg of grounded MOF powder and stirred for 30 min at room temperature in a magnetic stirrer at 600 rpm. The MOF-PCL solution was cast into a Teflon mold with a circumference of 11.62 cm and was left to dry at room temperature, to yield polymer-composite sheets (see Supplementary Figure S1).

2.5. Characterization. Fourier-Transformed Infrared (FTIR) spectra were recorded over the range of 600–4000 cm−1 using a Perkin Elmer Spectrum 100 FTIR spectrometer fitted with a PerkinElmer Universal ATR sampling device. Thermogravimetric analyses (TGA) were carried out using a Q5000IR thermogravimetric analyzer (TA Instruments, USA). Samples (ca. 5 mg) were heated in platinum pans from 30 to 700 °C at 5 °C min−1 under a nitrogen purge gas flow of 25 mL min−1. SEM images and energy dispersive X-ray (EDX) elemental analysis data were collected using an FEI Quanta 400 E-SEM instrument fitted with an Oxford Xplore30 EDS system. The samples were sputter-coated with gold using an Emitech K550 coating system and the analyses were carried out under vacuum. Information on the specific surface area and internal pore structure was obtained from N2 adsorption at 77 K on a Micromeritics 3Flex volumetric gas sorption analyzer. Each material (~60-80 mg) was degassed prior to the experiment (388 K, ~8 hrs, 1x10-6 mbar). Helium was used for free-space determination following isothermal data collection. N2 and Helium were supplied by Air Liquide and of purity 99.999%. Pore volume distribution as a function of pore width was calculated from the N2 adsorption data using a density functional theory (DFT) fitting and a cylindrical pore – NLDFT Tarazona Esf = 30 K model. The BET surface area was determined following the procedure outlined in ISO 9277[2]. A Rouquerol correction was applied to the BET fitting to calculate surface areas. A resultant correlation function of > 0.9999 was observed for each material and a positive intercept (Figure S4).

2.6. Loading Capacity. Loading capacity was determined using a method used by dos Reis et al., 2023 [26] with a slight modification. 5 mg of the loaded MOFs (see supplementary information for loading of 2,4-D and MCPA into the MOFs) was suspended into 3 mL of distilled water and sonicated for 60 min. After the sonication, 1 mL aliquot of solution was taken out and diluted with 2 mL of water. The concentration was measured using a UV–Vis spectrophotometer at 230 nm for 2,4-D and 227 nm for MCPA. The mass of herbicide released was determined from the volume, and the loading capacity in percentage was calculated using below Equation:

$$Loading\ Capacity\ (\%) = \frac{mass\ of herbicide}{mass\ of\ MOF}\ x\ 100$$

2.7. Release Study. For the release study, 5 mg of loaded MOFs and the MOF-PCL composite were submerged into 30 mL of deionized (DI) water at room temperature in a sealed container. 3 mL of the sample was collected from each set at different time intervals, at the same the stock was replaced by 3 mL of DI water to maintain the volume to 30 mL. 1 mL of the sample was added to a quartz cuvette with 2mL of water and the concentrations were calculated using UV-Vis spectrophotometer at 230 nm for 2,4-D and 227 nm for MCPA.

3. RESULTS AND DISCUSSION

Two iron-based MOFs, MIL-101(Fe) and NH2-MIL-101(Fe), were prepared via the solvothermal method. FeCl3 was added to 1,4-benzenedicarboxylic acid and 2-amino-1,4-benzenedicarboxylic acid, respectively using DMF at 110°C for 24 hours in 30 mL Teflon lined vials, following a previously reported procedure with a slight modification.[27] Following solvent exchange and drying, the activated MOFs were loaded with two different herbicides, 2,4-D and MCPA, by stirring the MOFs into the herbicide solution at 600 rpm for 3 days under ambient conditions. These loaded MOFs were subsequently incorporated into biodegradable polycaprolactone membranes via casting method and were studied for release of the herbicides till 216 h in an aqueous medium. For comparison, MOFs loaded with the herbicides were also investigated in parallel release studies.

3.1. Characterization of Fe-MOFs. The MOFs were characterized using PXRD, TGA, FT-IR, SEM and EDS. The PXRD patterns of MIL-101(Fe) and NH_2-MIL-101(Fe) were compared against the isostructural MIL-101(Cr), calculated from the previously reported single crystal data.[28, 29] The PXRD pattern of pristine MIL-101(Fe) aligns well with the reported PXRD of MIL-101(Cr). The high-intensity diffraction peaks at 2θ of 9.25, 10.49, 16.63, and 18.08 are also consistent with previously reported results for MIL-101(Fe).[30] For NH_2-MIL-101(Fe), two diffraction peaks similar to those of MIL-101(Fe) were observed at 9.36°, 16.86° and 18.99° in 2θ degrees.[30] In addition, the sharp peaks indicate the good crystallinity of both MIL-101(Fe) and NH_2-MIL-101(Fe). Similar findings have been reported in the literature, showing the high degree of crystallinity for MIL-101(Fe) and NH_2-MIL-101(Fe).[27, 30-33] On loading the herbicides, diminished intensity and broadening for the low angle peaks (such as at $2\theta = 11$) were observed which can be due to change in lattice or degradation of crystallinity as reported in other studies with MIL-101(Fe).[34, 35] The absence of the strong peaks around $2\theta = 16$ confirms that these peaks are not originating from particulate MCPA or 2,4-D (see Figure S2). In case of the PCL composites, the larger proportion of PCL reflects on the PXRD pattern where the other peaks are masked by the peaks originating from PCL, such as the strong peak at $2\theta = 21$ (see Figure S2 for PXRD of PCL).

The surface morphology of all the samples was investigated using SEM, corroborating with the PXRD results, and confirming the presence of MOF crystalline nature. SEM images in Figure 2 reveal that MIL-101(Fe) crystals have a typical octahedral shape (Figure 2a), whereas the synthesized NH_2-MIL-101(Fe) crystals have a hexagonal e morphology (Figure 2b).[30] The degradation of crystallinity observed in the powdered XRD was also evident in the morphology of 2,4-D and MCPA- loaded MIL-101(Fe) and NH_2-MIL-101(Fe) (Figure 2 c, d, e, and f). This could be caused by dissolution and mechanical stirring during the loading process. The SEM images (Figure 3, g - j), and EDS mapping (Figure S3) show a smooth homogeneous surface of the composites with uniform distribution of the Fe-MOFs.

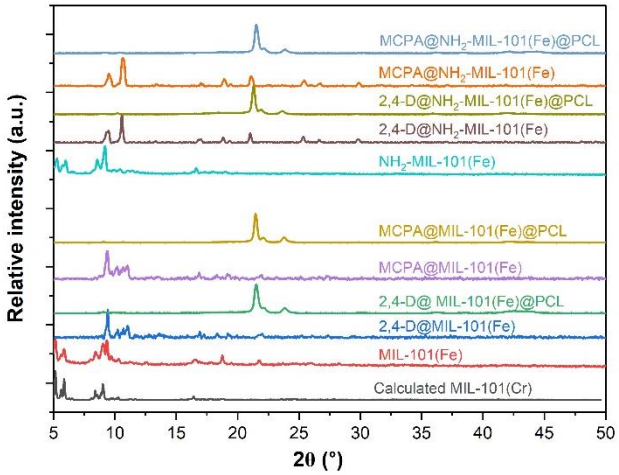

Figure 1. PXRD for calculated MIL-101(Cr), and experimentally measured for pristine and loaded MIL-101(Fe) and NH_2-MIL-101(Fe) samples, and their PCL composites.

The FTIR spectra of MIL-101(Fe) and NH_2-MIL-101(Fe) are consistent with spectra reported in previous literature[32, 36-39]. The peak between 1580–1660 cm−1 can be attributed to the symmetric C=O stretching of carboxylate groups coordinated to iron. Peaks at 1502 and 1580 cm−1 originate from the C=C stretching vibrations of the phenyl rings in the linker, while the peak at 770 cm-1 accounts for the C-H bending vibrations of the organic linker.

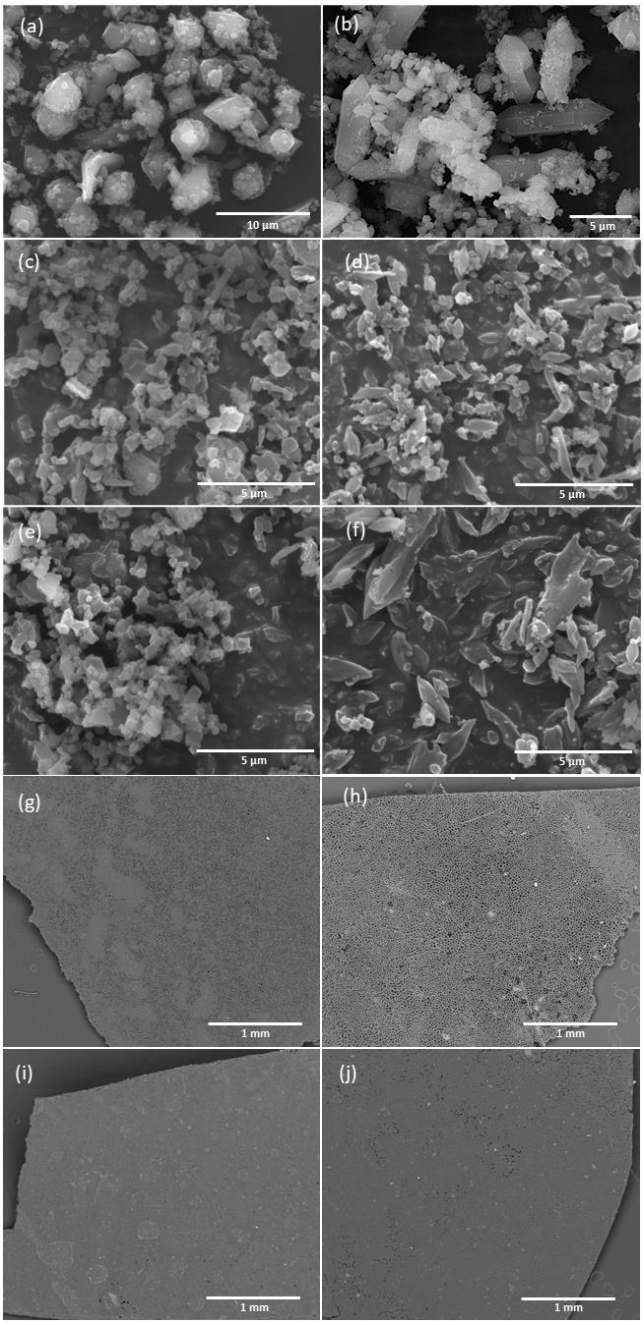

Figure 2. SEM images of a) MIL-101(Fe), b) NH_2-MIL-101(Fe), c) 2,4-D@MIL-101(Fe), d) 2,4-D@NH_2-MIL-101(Fe), e) MCPA@MIL-101(Fe), f) MCPA@NH_2-MIL-101(Fe), g) 2,4-D@MIL-101(Fe)@PCL, h) 2,4-D@NH_2-MIL-101(Fe)@PCL, i) MCPA@MIL-101(Fe)@PCL and j) MCPA@NH_2-MIL-101(Fe)@PCL. [Scale bar: (a) 10 µm, (b, c, d, e, f) 5 µm, and (g,h,i, j) 1 mm]

Compared to MIL-101(Fe), the amino-functionalised MIL-101(Fe) shows two characteristic peaks at 1255 and 1329 cm-1. These peaks account for the C-N stretching and N-H bending of the amino group in 2-amino-1,4-benzenedicarboxylic acid[36]. Broad peaks at 3469 and 3327 cm−1 in NH2-MIL-101(Fe) are attributed to the symmetric and asymmetric N−H bond stretching of primary amines, respectively[36, 39]. For the 2,4-D@MOF composite, bands at 1047 cm^{-1} and 1230 cm^{-1} indicate the presence of 2,4-D, corresponding to the C–O–C stretching of the ester group (Figure 3a).

In the case of MCPA@MIL-101(Fe), MCPA@NH_2- MIL-101(Fe), and their PCL composites, bands around 1193 cm^{-1} and 1056 cm^{-1} can be observed due to the C-O stretching (Figure 3b). The spectral band at 1568 cm^{-1}, attributed to the C=C stretching in MCPA, exhibits broadening in the MCPA@MOFs. This indicates a change in the chemical environment of MCPA within the MOF due to interactions with the MOF framework, indicating successful MCPA loading. When incorporating the herbicides@MOF into the PCL matrix, the peaks originating from the herbicides@MOFs are negligible compared to the peaks originating from the pure PCL (Figure S4). This is because the quantity of herbicide@MOFs is relatively very low compared to the amount of PCL in the composite, and therefore, the peaks corresponding to the herbicide@MOFs are masked by the peaks of the PCL. This finding also correlates with the PXRD data.

The thermal stability of all MOFs was studied under N_2 gas in detail,

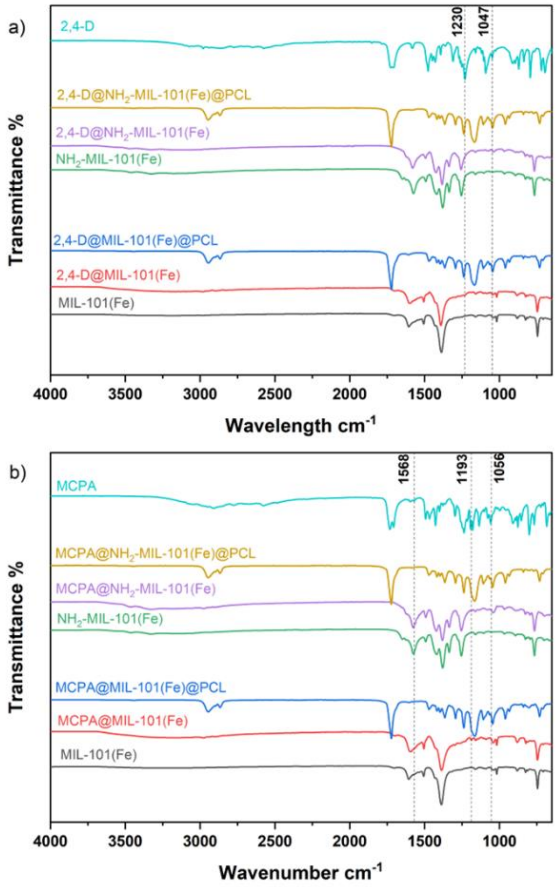

Figure 3. FTIR spectra of (a) MIL-101(Fe), NH_2-MIL-101(Fe) (pristine and loaded with 2,4-D), their PCL composites, and 2,4-D (b) MIL-101(Fe), NH_2-MIL-101(Fe) (pristine and loaded with MCPA), their PCL composites and MCPA

and the TGA plots are provided in the supplementary information (Figures S5). The decomposition of MOFs shows three stages of weight loss. The first weight loss below 150°C is due to the removal of water or solvent molecules occupying the pores and surfaces of the frameworks.[32] The second weight losses observed at temperature of 150-320°C, is due to the decomposition of the free organic structure present in the frameworks.[40] Subsequently, the loss after 320°C is attributed to the decomposition of the linker as a result of the breakdown of the framework.[41]

In the case of the herbicide-loaded samples, an additional weight loss stage was observed between 130 and 300 °C, attributed to volatilization and degradation of the herbicides.[41, 42] The final weight loss

occurred beyond 300°C, indicates the complete degradation resulting from linker degradation, leading to the collapse of the MOF structure.[41]

The TGA analyses of MOF-loaded PCL composites showed that PCL started to decompose at approximately 200 °C, leading to a substantial weight loss of ~90% for all the composites. The weight loss between 200-400°C is due to the degradation of the herbicides, and the organic structure of MOFs present in the PCL matrix. Beyond 400°C MOF@PCL composites shows a small weight loss due to the collapse of the MOF framework in the PCL matrix reaching a residual weight of ~5% for MOF loaded with 2,4-D and MCPA at 700 °C. This residual weight can be attributed to the presence of inorganic iron oxide resulting from the degradation of the MOFs.

N_2 gas sorption experiments were carried out at 77 K to determine surface area, pore volume and pore size distribution of the samples. The adsorption-desorption N_2 isotherms of the herbicide-loaded MOFs were compared against MIL-101(Fe) and NH_2-MIL-101(Fe) (Figure 4).

As classified by IUPAC[43], both pristine MOFs and herbicide loaded NH_2-MIL-101(Fe) MOFs exhibit type IV(b) isotherms, characteristic of materials exhibiting both micro and mesopores <4 nm in width. Both herbicide-loaded MIL-101(Fe) MOFs exhibit Type I isotherms indicating materials predominantly composed of micropores <2nm. This is consistent with the pore size distribution calculated for the native pristine samples, as illustrated in Figure 5. In comparison to the respective pristine MOFs, the herbicide-loaded MOFs exhibited a reduced quantity of adsorbed N_2, indicating decreased porosity. This reduction is further evidenced by the diminished surface areas (SA) and total pore volumes (TPV) observed for the MOF samples, as summarised in Table 1. Surface area measurements were performed for each sample and fitted using the Rouquerol method[44] with a positive y-intercept and the highest R^2 values (Figure S6).

Table 1. Pore Characteristics of the Iron-based MOF Samples

Sample ID	BET Surface area (m^2g^{-1})	Total Pore volume (TPV)[a] (cm^3g^{-1})	Micro and mesopore Volume[b] (cm^3g^{-1})	Pore volume reduction (%)[c]b
MIL-101(Fe)	1397± 2.03#	0.69	0.74	--
NH_2-MIL-101(Fe)	1300± 3.9	0.67	0.67	--
2,4-D@MIL-101(Fe)	424. ± 0.5	0.21	0.21	69
MCPA@MIL-101(Fe)	562 ± 0.4	0.26	0.27	62
2,4-D@NH_2-MIL-101(Fe)	345 ± 0.9	0.20	0.17	70
MCPA@NH_2-MIL-101(Fe)	308 ± 1.8	0.15	0.14	77

[a] Single point adsorption total pore volume of pores taken at p/p_o = 0.94; [b] DFT cumulative pore volume of pores <52 Å [c] with respect to the pristine MOFs; # the standard deviation for the BET surface area is from 3flex fitting calculation.

Comparing the SA and TPV of 2,4-D@MOFs and MCPA@MOFs to MIL-101(Fe) and NH_2-MIL-101(Fe), it was found that (a) 2,4-D@MIL-101(Fe) observed a 70% reduction in SA and 69% reduction in TPV in comparison to MIL-101(Fe); (b) MCPA@MIL-101(Fe) observed a 60% decrease in SA and 62% reduction in TPV in comparison to MIL-101(Fe); (c) 2,4-D@NH_2-MIL-101(Fe) observed a 73% reduction in SA and 70% increase in TPV in comparison to NH_2-MIL-101(Fe) and (d) MCPA@NH_2-MIL-101(Fe) observed a 76 % decrease in SA and 77% decrease in TPV in comparison to NH_2-MIL-101(Fe).

The reduction in total pore volume and surface area could be due to 2,4-D and MCPA occupying the available pore volume or to losses in MOF crystallinity during the loading process, as was observed in the PXRD data (Figure 1).

To further elucidate the effect of herbicide infiltration, pore size distributions & cumulative pore volumes were calculated by fitting the isotherms to DFT models. These results are compared against pristine MOFs (Figure 5). Changes in the pore network and available volume within the individual pores of the samples reveal whether they are occupied/ blocked with molecules or if any changes in pore sizes occurred during processing.

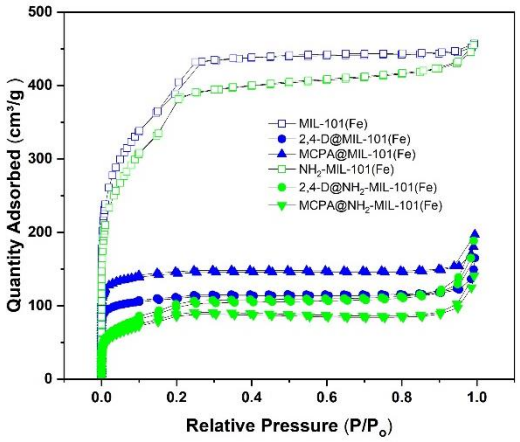

Figure 4. Nitrogen adsorption-desorption isothermal cycles at 77 K of Fe-MOF samples used in this work.

Across all samples, the most significant reduction in available pore volume was observed in the mesopores, with up to a 97% reduction in the available pore volume in the 30.6 Å pore for MIL-101(Fe) after the introduction of 2,4-D. A significant reduction in micropore volume was observed for the amino-functionalized MOF (Table S2). However, in MIL-101(Fe), the smallest pore (5.9Å) showed no significant losses, indicating that the pesticide molecules did not occupy these pores.

In addition, the introduction of herbicides into the MOFs led to changes in the width of available pores (Table S3), indicating alterations to the MOF structure. The most significant changes were observed for MCPA@MIL-101(Fe), with up to a 40% reduction in mesopore width. The results suggest that the herbicides chiefly accumulate in the mesopores of the samples, reducing the available pore volume for nitrogen molecules to occupy. The presence of amino-functional groups in the MOFs appears to enhance the infiltration of pesticide molecules into the micropores, thus increasing the storage capacity of the MOF.

3.2. Loading and Release Study. PXRD, FTIR, SEM and elemental mapping confirmed the successful loading of 2,4-D and MCPA into the two MOFs. The loading capacity for the herbicides in the MOFs was estimated by suspending the loaded MOFs with distilled water and sonicating for 60 minutes. The loading capacities were found to be 18.06% for 2,4-D@MIL-101(Fe) and 21.51% for MCPA@MIL-101(Fe). In contrast, the loading capacities were 26.61% for 2,4-

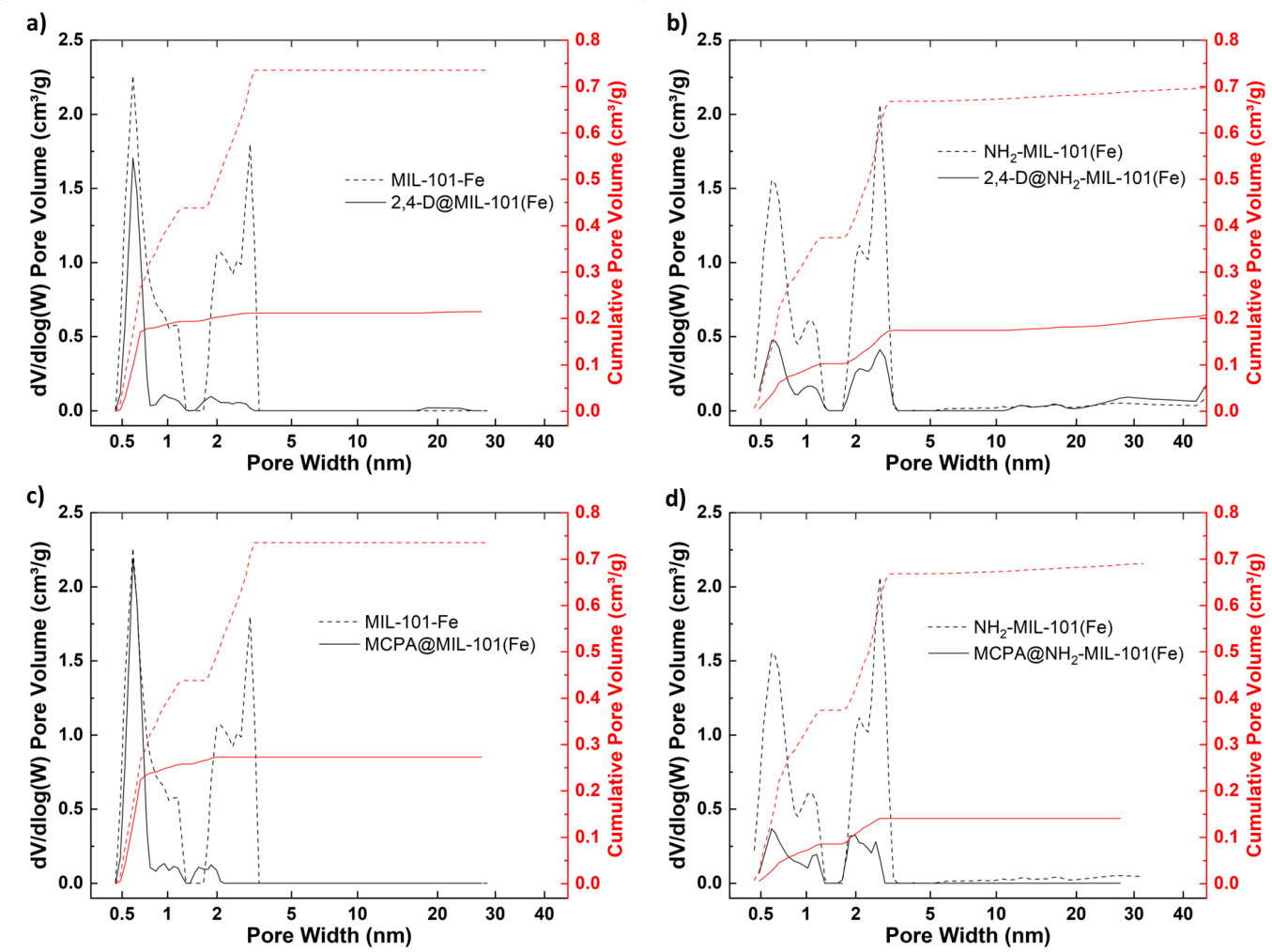

Figure 5. a)-d) Pore size distribution and cumulative pore volume of MOF samples, from 77 K N_2 sorption data fitted with a Tarazona cylindrical pore NLDFT model.

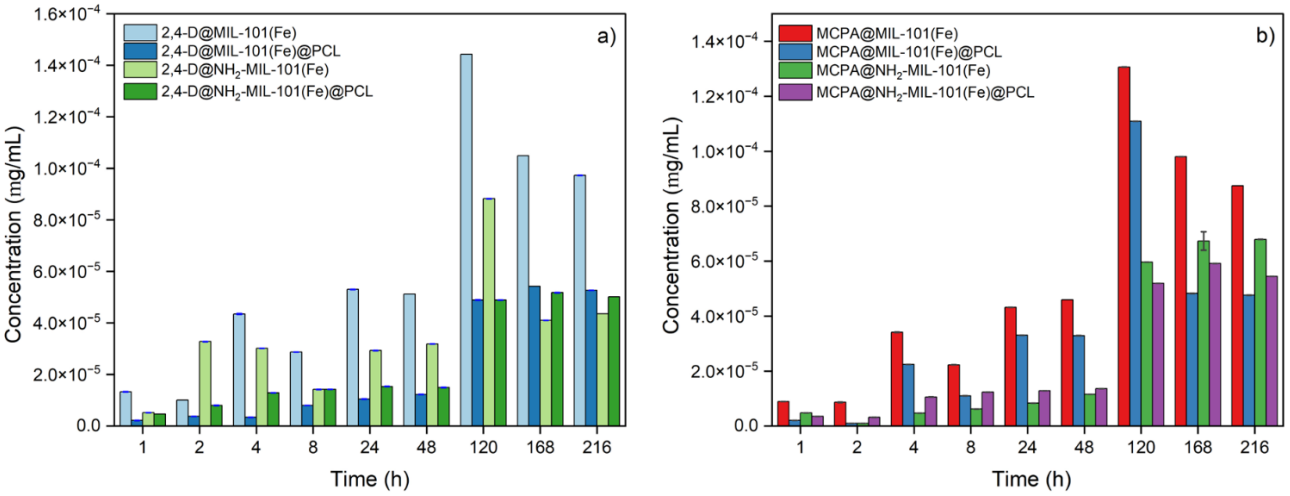

Figure 6. Release study of a) 2,4-D and b) MCPA from MIL-101(Fe), NH_2-MIL-101(Fe), and their PCL composites in water for over time

D@NH_2-MIL-101(Fe), and 23.32% for MCPA@NH_2-MIL-101(Fe). The higher loading capacity for the amino-functionalized MOF can be attributed to hydrogen bonding between the NH_2- group of NH_2-MIL-101(Fe) and the carboxylate and chloride groups of 2,4-D and MCPA. This is further supported by the greater loss in pore volume for the loaded NH_2-MIL-101(Fe). All sets of 2,4-D and MCPA-loaded MOFs and their PCL composites were immersed in 30 mL distilled water at room temperature for 216 h. The filtered aliquots were analyzed using

a UV-visible spectrophotometer to quantify the amount of 2,4-D and MCPA released from the MOFs and their PCL composite. As shown in Figure 6, for both the 2,4-D and MCPA loaded MOFs, the release of the herbicide in water was faster compared to the PCL composites, with maximum values of 1.44 x 10-4 mg mL-1 and 8.82 x 10-5 mg mL-1 for 2,4-D@MIL-101(Fe) and 2,4-D@NH2-MIL-101(Fe), respectively. For MCPA@MIL-101(Fe) and MCPA@NH2-MIL-101(Fe), the values were 1.31 x 10-4 mg mL-1 and 6.79 x 10-5 mg mL-1, respectively. The higher release of herbicides from both the MOFs may be because of the herbicides binding loosely to the MOF, allowing for faster diffusion from the pores. Furthermore, comparing NH_2-MIL-101(Fe) to MIL-101(Fe) loaded with 2,4-D and MCPA, the herbicide-loaded MIL-101(Fe) shows higher release rates beyond 120 h. This difference can be attributed to MIL-101(Fe) providing fewer binding sites for the herbicides compared to NH_2-MIL-101(Fe), facilitating faster diffusion from its structure.

However, for NH_2-MIL-101(Fe), the herbicide release was slightly reduced due to weak H-bonding between the NH_2- group of NH_2-MIL-101(Fe) and the carboxylate group of 2,4-D and MCPA. Recent release studies of 2,4-D and MCPA using Zr-based MOFs (UiO-66 and UiO-66-NH_2) showed that in general amino-functionalized UiO-66 exhibits a slower release than UiO-66 due to hydrogen bond interactions between the carboxylate group of the 2,4-D and ─NH_2 groups of UiO-66-NH_2.[26, 39].

When the herbicide@MOFs were incorporated into the PCL matrix, the herbicide release was more controlled. For instance, the amount of 2,4-D released from 50 mg of MOF-loaded PCL composite (containing 5 mg of herbicide@MOFs) was 5.42 x 10^{-5} mg mL^{-1} for 2,4-D@MIL-101(Fe)@PCL and 5.17 x 10^{-5} mg mL^{-1} much more controlled compared to the powder form (1.44 x 10^{-4} mg mL^{-1} and 8.82 x 10^{-5} mg mL^{-1} for 2,4-D@MIL-101(Fe) and 2,4-D@NH_2- MIL-101(Fe) respectively. Similar patterns were observed for MCPA in the iron-MOF PCL composites, with release values of 4.83 x 10^{-5} mg mL^{-1} and 5.91 x 10^{-5} mg mL^{-1} for MCPA@MIL-101(Fe)@PCL and MCPA@NH_2-MIL-101(Fe)@PCL, respectively. In both cases, MIL-101(Fe) showed faster herbicide release compared to NH_2-MIL-101(Fe). This correlates to the hypothesis that the carboxylate group in 2,4-D and MCPA interacts with the amino group of the NH_2- MIL-101(Fe) via hydrogen bonding, leading to slower release of the herbicides.

It was also observed that for herbicide@MOF the release of herbicide decreases after 120 h. As discussed above the structure of the MOF degrades over time with possible formation of iron oxo and hydroxo complexes which is evident from the XRD patterns of the loaded MOFs where numerous small peaks, characteristic of α-FeO(OH) were observed.[45] From earlier studies α-FeO(OH) is also reported to be the one of the best sorbents for phenoxy acid herbicides (in this case 2,4-D and MCPA).[46] Thus, the decrease of the release after 120 h is potentially due to the interaction of α-FeO(OH) with the herbicides to form outer-sphere and inner sphere complexes as reported by Kersten *et al.*[46]

To understand the interactions between the MOFs and herbicides in more details computational studies were performed (see SI for details). The results indicate the formation of hydrogen bonds between the amino group of NH_2-MIL-101(Fe) and the carboxylate group of the 2,4-D and MCPA molecules, consistent with the slower release observed for the NH2-MIL-101(Fe). The binding energy was found to be -203.99 kJ mol−1 for the interaction between 2,4-D and NH2-MIL-101(Fe), which is 45% higher than binding energy for the interaction between 2,4-D and MIL-101(Fe) (Figure 7). Similarly, the binding energy was -198.73 kJ mol-1 for the interaction between MCPA with NH2-MIL-101(Fe), 22% higher than for MIL-101(Fe). The higher binding energy for 2,4-D with NH2-MIL-101(Fe) compared to the interaction of MCPA with the same Fe-MOF is likely to be due to more extensive interactions of 2,4-D molecule via two -Cl groups and ─COOH group, as opposed to MCPA, which has only one chloride group. The two chloride groups, along with the ─COOH group, actively form hydrogen bonds with the amino group of the linker.

For 2,4-D@MIL-101(Fe), a π-stacking distance of 3.42 Å was observed between the linker of MIL-101(Fe) and the phenyl ring of 2,4-D. The H-bond lengths was measured as 2.062 Å for Cl•••HOH (metal cluster cap) and 1.866 Å for H•••HOH (metal cluster cap). In contrast, no π-stacking was observed for MCPA@MIL-101(Fe), with a hydrogen bond length of 2.010 Å between MCPA and MIL-101(Fe). In the case of NH_2-MIL-101(Fe), a slight offset π-stacking of 3.87 Å was observed between the linker of NH_2-MIL-101(Fe) and the phenyl ring of 2,4-D. The H-bond lengths were measured as 2.171 Å for O•••HN-H (linker of the MOF) and 1.425 Å for OH•••NH_2 (linker of the MOF). For MCPA@NH_2-MIL-101(Fe), a π-stacking distance of 3.44 Å was observed between the linker and the phenyl ring, with a H-bond length of 1.475 Å between MCPA's OH•••NH_2(linker). These results indicate that NH_2-MIL-101(Fe) use more H-bonding and π-stacking interactions to tightly bind the herbicides to the pore walls. However, in the case of MCPA@MIL-101(Fe), MCPA is loosely held, occupying the centre of the pore and blocking it.

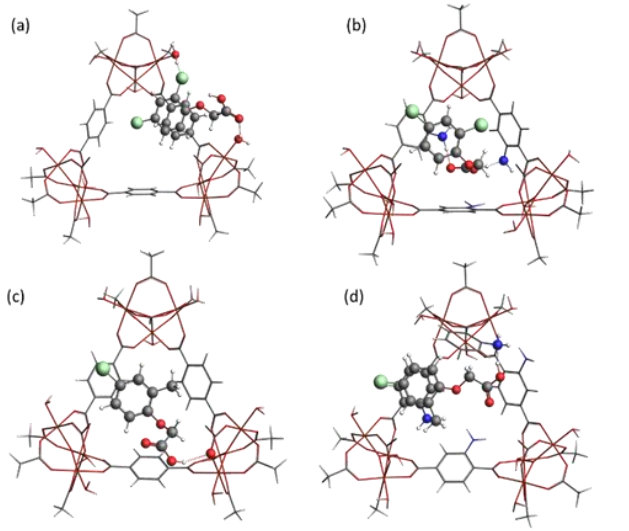

Figure 7. Model showing the interaction of 2,4-D with (a) MIL-101(Fe) (b) NH_2- MIL-101(Fe) and MCPA with (c) MIL-101(Fe) (d) NH_2- MIL-101(Fe).

CONCLUSIONS

This study has shown potential applications of two iron-based MOFs, namely MIL-101(Fe) and NH_2-MIL-101(Fe), for sustainable delivery of two widely used herbicides, 2,4-D and MCPA. Comprehensive characterizations confirmed the synthesis of MIL-101(Fe) and NH_2-MIL-101(Fe) and loading of both MOFs with the two herbicides. Despite high herbicide loading capacities, PXRD revealed broadening of diffraction peaks which was attributed to the partial degradation and loss of crystallinity of the MOFs during the loading process. It should be noted that in contrast to many other applications of MOFs, degradation of the MOFs is a desired outcome towards the end of their use in agrochemical applications. The herbicide-loaded MOFs were incorporated into biodegradable polycaprolactone (PCL) membrane to develop hybrid composites. The release rates of 2,4-D and MCPA from both MIL-101(Fe) and NH_2-MIL-101(Fe), as well as their respective PCL composites, were thoroughly investigated. The results indicate a controlled and gradual release of the herbicides when incorporated into PCL, suggesting sustainable and long-lasting release profiles suitable for agricultural applications. These MOF-polymer composites hold promise for controlled and sustainable delivery of pesticides and other agrochemicals, thereby preventing their overuse. Moreover, the use of the iron-based MOFs not only contributes to the controlled release of herbicides but also can be a potential source of iron as a micronutrient for plants upon degradation. This dual functionality can potentially enhance the environmental friendliness and sustainability of the composites. Further studies are currently underway to

understand the time-dependent degradation of these MOFs and their effect on broadleaf weeds and plant growth.

ASSOCIATED CONTENT

Supporting Information

The supporting information contains additional optical and SEM images, elemental mapping, PXRD plots, IR spectra, BET and pore size distribution plots, TGA plots, and DFT data.

The Supporting Information is available free of charge on the ACS Publications website.

AUTHOR INFORMATION

Corresponding Author

*** Sanjit Nayak** - Bristol Composites Institute, School of Civil, Aerospace and Design Engineering, University of Bristol, Bristol, BS8 1TR, United Kingdom; Email: s.nayak@bristol.ac.uk

***Valeska P. Ting**- Research School of Chemistry, Australian National University, Canberra ACT 2601 Australia; E-mail: valeska.ting@anu.edu.au

Authors

Parimal C. Bhomick - Bristol Composites Institute, University of Bristol, Bristol, BS8 1TR, UK; Department of Chemistry, St Joseph University, Chumoukedima, 797115, Nagaland, India

Evdokiya H. Ivanovska- School of Archaeological and Forensic Sciences, University of Bradford, Bradford, West Yorkshire, BD7 1DP, UK

Lila A. M. Mahmoud - Bristol Composites Institute, University of Bristol, Bristol, BS8 1TR, UK; School of Chemistry, University of Bristol, Bristol, BS8 1TS, UK

Huan V. Doan- Research School of Chemistry, Australian National University, Canberra ACT 2601 Australia

Lui R. Terry - Bristol Composites Institute, University of Bristol, Bristol, BS8 1TR, UK; School of Civil, Aerospace and Design Engineering, University of Bristol, Bristol, BS8 1TR, UK

Matthew A. Addicoat - School of Science and Technology, Nottingham Trent University, Clifton Lane, Nottingham NG11 8NS, UK

Jemma L. Rowlandson - Bristol Composites Institute, University of Bristol, Bristol, BS8 1TR, UK; School of Electrical, Electronic and Mechanical Engineering, University of Bristol, Bristol, BS8 1TR, UK

Sebastien Rochat- School of Chemistry, University of Bristol, Bristol, BS8 1TS, UK; School of Engineering Mathematics and Technology, University of Bristol, Bristol, BS8 1TR, UK

Author Contributions

P.C.B.: Implementation of idea, experiments, materials characterization, preparation of manuscript. E.H.I.: Experiment, materials characterization. L.A.M.M.: Experiment, materials characterization. H.V.D.: Investigation (materials characterization) analysis, review and editing manuscript. L.R.S.: Investigation (materials characterization) analysis, review and editing manuscript. M.A.A.: Computational studies, review and editing of manuscript. J.L.R.: Supervision, review and editing of manuscript. S.R.: Supervision, review and editing of manuscript. V.P.T.: Supervision, review and editing of manuscript. S.N.: Project lead, conceptualization, supervision, materials characterization, review, editing and submission of manuscript.

Notes

The authors declare no competing financial interest.

ACKNOWLEDGMENT

VPT thanks the Engineering and Physical Sciences Research Council (EPSRC) for funding *via* an EPSRC Research Fellowship (EP/R01650X/1). P.B. acknowledges funding from the SERB International Research Experience (SIRE) Programme (SIR/2022/001019) by the Science and Engineering Research Board, New Delhi, India.

ABBREVIATIONS

2,4-D, 2,4-dichlorophenoxyacetic acid; BET, Brunauer−Emmett−Teller; IR, infrared; MCPA, 2-methyl-4chlorophenoxyacetic acid; MOF, Metal Organic Frameworks; PCL, polycaprolactone; PXRD, powder X-ray diffraction; SEM, scanning electron microscope; TGA, thermogravimetric analysis

REFERENCES

(1) Tudi, M.; Daniel Ruan, H.; Wang, L.; Lyu, J.; Sadler, R.; Connell, D.; Chu, C.; Phung, D. T. Agriculture Development, Pesticide Application and Its Impact on the Environment. Int J Environ Res Public Health 2021, 18 (3), 1112. DOI: 10.3390/ijerph18031112.

(2) Lewis, K. A.; Tzilivakis, J.; Warner, D. J.; Green, A. An international database for pesticide risk assessments and management. Human and Ecological Risk Assessment: An International Journal 2016, 22 (4), 1050-1064. DOI: 10.1080/10807039.2015.1133242.

(3) Pesticide Properties DataBase. University of Hertfordshire, 2024. https://sitem.herts.ac.uk/aeru/ppdb/en/atoz.htm (accessed 2024 11 Jan).

(4) Zilberman, D.; Schmitz, A.; Casterline, G.; Lichtenberg, E.; Siebert, J. B. THE ECONOMICS OF PESTICIDE USE AND REGULATION. Science 1991, 253 (5019), 518-522, Article. DOI: 10.1126/science.253.5019.518.

(5) Dhananjayan, V.; Jayakumar, S.; Ravichandran, B. Conventional Methods of Pesticide Application in Agricultural Field and Fate of the Pesticides in the Environment and Human Health. In Controlled Release of Pesticides for Sustainable Agriculture, K. R, R., Thomas, S., Volova, T., K, J. Eds.; Springer International Publishing, 2020; pp 1-39.

(6) van den Berg, F.; Kubiak, R.; Benjey, W. G.; Majewski, M.; Yates, Sr.; Reeves, G. L.; Smelt, J.; van der Linden, A. Emission of Pesticides into the Air. Water, Air and Soil Pollution 1999, 115 (1-4), 195-218. DOI: http://dx.doi.org/10.1023/A:1005234329622 ABI/INFORM Collection.

(7) Pimentel, D. Amounts of pesticides reaching target pests: Environmental impacts and ethics. Journal of Agricultural and Environmental Ethics 1995, 8 (1), 17-29. DOI: 10.1007/bf02286399.

(8) Annett, R.; Habibi, H. R.; Hontela, A. Impact of glyphosate and glyphosate-based herbicides on the freshwater environment. J. Appl. Toxicol. 2014, 34 (5), 458-479, Review. DOI: 10.1002/jat.2997.

(9) Mann, R. M.; Hyne, R. V.; Choung, C. B.; Wilson, S. P. Amphibians and agricultural chemicals: Review of the risks in a complex environment. Environ. Pollut. 2009, 157 (11), 2903-2927, Review. DOI: 10.1016/j.envpol.2009.05.015.

(10) Haynes, D.; Muller, J.; Carter, S. Pesticide and herbicide residues in sediments and seagrasses from the Great Barrier Reef world heritage area and Queensland coast. Mar. Pollut. Bull. 2000, 41 (7-12), 279-287, Article. DOI: 10.1016/s0025-326x(00)00097-7.

(11) Mahmoud, L. A. M.; Dos Reis, R. A.; Chen, X.; Ting, V. P.; Nayak, S. Metal-Organic Frameworks as Potential Agents for Extraction and Delivery of Pesticides and Agrochemicals. ACS Omega 2022, 7 (50), 45910-45934. DOI: 10.1021/acsomega.2c05978.

(12) Dehghani, M. H.; Ahmadi, S.; Ghosh, S.; Khan, M. S.; Othmani, A.; Khanday, W. A.; Gökkuş, Ö.; Osagie, C.; Ahmaruzzaman, M.; Mishra, S. R.; et al. Sustainable remediation technologies for removal of pesticides as organic micro-pollutants from water environments: A review. Applied Surface Science Advances 2024/02/01, 19. DOI: 10.1016/j.apsadv.2023.100558.

(13) Li, J.; Lv, Q.; Bi, L.; Fang, F.; Hou, J.; Di, G.; Wei, J.; Wu, X.; Li, X. Metal-organic frameworks as superior adsorbents for pesticide removal from water: The cutting-edge in characterization, tailoring, and application potentials. Coordination Chemistry Reviews 2023/10/15, 493. DOI: 10.1016/j.ccr.2023.215303.

(14) Alrowais, R.; daiem, M. M. A.; Nasef, B. M.; Said, N.; Alrowais, R.; Abdel daiem, M. M.; Nasef, B. M.; Said, N. Activated Carbon Fabricated from Biomass for Adsorption/Bio-Adsorption of 2,4-D and MCPA: Kinetics, Isotherms, and Artificial Neural Network Modeling. Sustainability 2024, Vol. 16, Page 299 2023-12-28, 16 (1). DOI: 10.3390/su16010299.

(15) Rojas, S.; Rodriguez-Dieguez, A.; Horcajada, P. Metal-Organic Frameworks in Agriculture. ACS Appl Mater Interfaces 2022, 14 (15), 16983-17007. DOI: 10.1021/acsami.2c00615.

(16) Wu, K.; Xu, X.; Ma, F.; Du, C. Fe-Based Metal-Organic Frameworks for the Controlled Release of Fertilizer Nutrients. ACS Omega 2022, 7 (40), 35970-35980. DOI: 10.1021/acsomega.2c05093.

(17) Maksimchuk, N. V.; Zalomaeva, O. V.; Skobelev, I. Y.; Kovalenko, K. A.; Fedin, V. P.; Kholdeeva, O. A. Metal–organic frameworks of the MIL-101 family as heterogeneous single-site catalysts. Proceedings of the Royal Society A: Mathematical, Physical and Engineering Sciences 2012, 468 (2143), 2017-2034. DOI: 10.1098/rspa.2012.0072.

(18) Shin, J.; Kim, M.; Cirera, J.; Chen, S.; Halder, G. J.; Yersak, T. A.; Paesani, F.; Cohen, S. M.; Meng, Y. S. MIL-101(Fe) as a lithium-ion battery electrode material: a relaxation and intercalation mechanism during lithium insertion. Journal of Materials Chemistry A 2015, 3 (8), 4738-4744. DOI: 10.1039/c4ta06694d.

(19) Karimi Alavijeh, R.; Akhbari, K. Biocompatible MIL-101(Fe) as a Smart Carrier with High Loading Potential and Sustained Release of Curcumin. Inorg Chem 2020, 59 (6), 3570-3578. DOI: 10.1021/acs.inorgchem.9b02756.

(20) Almáši, M.; Zeleňák, V.; Palotai, P.; Beňová, E.; Zeleňáková, A. Metal-organic framework MIL-101(Fe)-NH2 functionalized with different long-chain polyamines as drug delivery system. Inorganic Chemistry Communications 2018, 93, 115-120. DOI: 10.1016/j.inoche.2018.05.007.

(21) Nuruzzaman, M.; Rahman, M. M.; Liu, Y. J.; Naidu, R. Nanoencapsulation, Nano-guard for Pesticides: A New Window for Safe Application. J. Agric. Food Chem. 2016, 64 (7), 1447-1483, Review. DOI: 10.1021/acs.jafc.5b05214.

(22) Livesey, T. C.; Mahmoud, L. A. M.; Katsikogianni, M. G.; Nayak, S.; Livesey, T. C.; Mahmoud, L. A. M.; Katsikogianni, M. G.; Nayak, S. Metal–Organic Frameworks and Their Biodegradable Composites for Controlled Delivery of Antimicrobial Drugs. Pharmaceutics 2023, Vol. 15, Page 274 2023-01-12, 15 (1). DOI: 10.3390/pharmaceutics15010274.

(23) Shabaev, A. R.; Kanonykina, A. Y.; Bogdanov, L. A.; Shishkova, D. K.; Kudryavtseva, Y. A. Selection of Polymer for Stent-Graft Coating in Terms of Biocompatibility and Biodegradation Characteristics. Complex Issues of Cardiovascular Diseases 2025, 13 (4), 77-89. DOI: 10.17802/2306-1278-2024-13-4-77-89.

(24) Ali, S. F. A.; Ali, S. F. A. Mechanical and thermal properties of promising polymer composites for food packaging applications. IOP Conference Series: Materials Science and Engineering 2016-07-01, 137 (1). DOI: 10.1088/1757-899X/137/1/012035.

(25) Deshpande, M. V.; Girase, A.; King, M. W.; Deshpande, M. V.; Girase, A.; King, M. W. Degradation of Poly(ε-caprolactone) Resorbable Multifilament Yarn under Physiological Conditions. Polymers 2023, Vol. 15, Page 3819 2023-09-19, 15 (18). DOI: 10.3390/polym15183819.

(26) Reis, R. A. d.; Mahmoud, L. A. M.; Ivanovska, E. H.; Telford, R.; Addicoat, M. A.; Terry, L. R.; Ting, V. P.; Nayak, S. Biodegradable Polymer-Metal-Organic Framework (MOF) Composites for Controlled and Sustainable Pesticide Delivery. Advanced Sustainable Systems 2023, 7 (12). DOI: 10.1002/adsu.202300269.

(27) Qin, L. Z.; Xiong, X. H.; Wang, S. H.; Zhang, L.; Meng, L. L.; Yan, L.; Fan, Y. N.; Yan, T. A.; Liu, D. H.; Wei, Z. W.; et al. MIL-101-Cr/Fe/Fe-NH(2) for Efficient Separation of CH(4) and C(3)H(8) from Simulated Natural Gas. ACS Appl Mater Interfaces 2022, 14 (40), 45444-45450. DOI: 10.1021/acsami.2c13446.

(28) Lebedev, O. I.; Millange, F.; Serre, C.; Van Tendeloo, G.; Férey, G. First direct imaging of giant pores of the metal-organic framework MIL-101. Chem. Mater. 2005, 17 (26), 6525-6527. DOI: 10.1021/cm051870o.

(29) Férey, G.; Mellot-Draznieks, C.; Serre, C.; Millange, F.; Dutour, J.; Surblé, S.; Margiolaki, I. A chromium terephthalate-based solid with unusually large pore volumes and surface area. Science 2005, 309 (5743), 2040-2042. DOI: 10.1126/science.1116275.

(30) Gecgel, C.; Simsek, U. B.; Gozmen, B.; Turabik, M. Comparison of MIL-101(Fe) and amine-functionalized MIL-101(Fe) as photocatalysts for the removal of imidacloprid in aqueous solution. J IRAN CHEM SOC 2019, 16 (8), 1735-1748. DOI: 10.1007/s13738-019-01647-w.

(31) Wang, Y.; Guo, W.; Li, X. Activation of persulfates by ferrocene–MIL-101(Fe) heterogeneous catalyst for degradation of bisphenol A. RSC Adv. 2018, 8 (64), 36477-36483. DOI: 10.1039/C8RA07007E.

(32) Shan, Y.; Xu, C.; Zhang, H.; Chen, H.; Bilal, M.; Niu, S.; Cao, L.; Huang, Q. Polydopamine-Modified Metal–Organic Frameworks, NH2-Fe-MIL-101, as pH-Sensitive Nanocarriers for Controlled Pesticide Release. Nanomaterials 2020, 10 (10), 2000. DOI: 10.3390/nano10102000.

(33) Jia, D.; Li, Y.; Cai, H.; Duan, Y.; Li, J.; Ling, C. MIL-101(Fe) Metal–Organic Framework Nanoparticles Functionalized with Amino Groups for Cr(VI) Capture. Acs Appl Nano Mater 2023, 6 (8), 6820-6830. DOI: 10.1021/acsanm.3c00544.

(34) Shi, H.; Gu, Z.; Han, M.; Chen, C.; Chen, Z.; Ding, J.; Wang, Q.; Wan, H.; Guan, G. Preparation of heterogeneous interfacial catalyst benzimidazole-based acid ILs@MIL-100(Fe) and its application in esterification. Colloids and Surfaces A: Physicochemical and Engineering Aspects 2021, 608. DOI: 10.1016/j.colsurfa.2020.125585.

(35) Canioni, R.; Roch-Marchal, C.; Sécheresse, F.; Horcajada, P.; Serre, C.; Hardi-Dan, M.; Férey, G.; Grenèche, J.-M.; Lefebvre, F.; Chang, J.-S.; et al. Stable polyoxometalate insertion within the mesoporous metal organic framework MIL-100(Fe). Journal of Materials Chemistry 2011/01/10, 21 (4). DOI: 10.1039/C0JM02381G.

(36) Xie, Q.; Li, Y.; Lv, Z.; Zhou, H.; Yang, X.; Chen, J.; Guo, H. Effective Adsorption and Removal of Phosphate from Aqueous Solutions and Eutrophic Water by Fe-based MOFs of MIL-101. Sci Rep 2017, 7 (1), 3316. DOI: 10.1038/s41598-017-03526-x.

(37) Zhang, X.; Yu, R.; Wang, D.; Li, W.; Zhang, Y. Green Photocatalysis of Organic Pollutants by Bimetallic Zn-Zr Metal-Organic Framework Catalyst. Frontiers in Chemistry 2022, 10, 918941. DOI: 10.3389/fchem.2022.918941.
(38) Kim, H.-G.; Choi, K.; Lee, K.; Lee, S.; Jung, K.-W.; Choi, J.-W. Controlling the Structural Robustness of Zirconium-Based Metal Organic Frameworks for Efficient Adsorption on Tetracycline Antibiotics. Water 2021, 13 (13), 1869. DOI: 10.3390/w13131869.
(39) Mahmoud, L. A. M.; Telford, R.; Livesey, T. C.; Katsikogianni, M.; Kelly, A. L.; Terry, L. R.; Ting, V. P.; Nayak, S. Zirconium-Based MOFs and Their Biodegradable Polymer Composites for Controlled and Sustainable Delivery of Herbicides. Acs Appl Bio Mater 2022, 5 (8), 3972-3981. DOI: 10.1021/acsabm.2c00499.
(40) Gusain, D.; Awolusi, O. O.; Bux, F. Synthesis and characterization of iron oxide/MIL-101 composite via microwave solvothermal treatment. Surface Science 2022, 716. DOI: 10.1016/j.susc.2021.121952.
(41) Liu, Z.; He, W.; Zhang, Q.; Shapour, H.; Bakhtari, M. F. Preparation of a GO/MIL-101(Fe) Composite for the Removal of Methyl Orange from Aqueous Solution. ACS Omega 2021, 6 (7), 4597-4608. DOI: 10.1021/acsomega.0c05091.
(42) Hasanuddin, N. I.; Dzulkifli, N. N.; Sarijo, S. H.; Ghazali, S. A. I. S. M. Physicochemical Characterization and Controlled Release Formulation on Intercalated 2-Methyl-4-chlorophenoxy Acetic Acid-Graphite Oxide (MCPA-GO) Nanocomposite. Indonesian Journal of Chemistry 2020, 20 (2), 299-306. DOI: https://doi.org/10.22146/ijc.40921.
(43) Thommes, M.; Kaneko, K.; Neimark, A. V.; Olivier, J. P.; Rodriguez-Reinoso, F.; Rouquerol, J.; Sing, K. S. W. Physisorption of gases, with special reference to the evaluation of surface area and pore size distribution (IUPAC Technical Report). Pure and Applied Chemistry 2015, 87 (9-10), 1051-1069. DOI: 10.1515/pac-2014-1117.
(44) J. Rouquerol, F. R., P. Llewellyn, G. Maurin, K.S.W. Sing. Adsorption by Powders and Porous Solids; Elsevier Science & Technology, 2014. DOI: 10.1016/c2010-0-66232-8.
(45) Liu, X.; Qiu, G.; Yan, A.; Wang, Z.; Li, X. Hydrothermal synthesis and characterization of α-FeOOH and α-Fe2O3 uniform nanocrystallines. Journal of Alloys and Compounds 2007/05/16, 433 (1-2). DOI: 10.1016/j.jallcom.2006.06.029.
(46) Kersten, M.; Tunega, D.; Georgieva, I.; Vlasova, N.; Branscheid, R. Adsorption of the herbicide 4-chloro-2-methylphenoxyacetic acid (MCPA) by goethite. Environ Sci Technol 2014, 48 (20), 11803-11810. DOI: 10.1021/es502444c From NLM Medline.

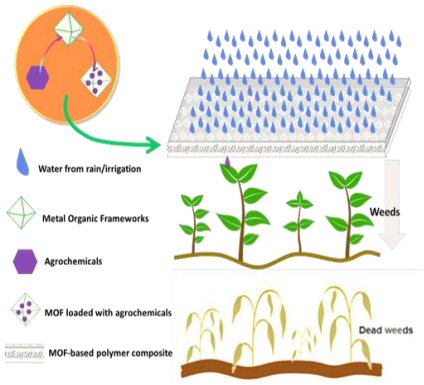
Water from rain/irrigation
Metal Organic Frameworks
Agrochemicals
MOF loaded with agrochemicals
MOF-based polymer composite
Weeds
Dead weeds